MethodsX 8 (2021) 101368

Contents lists available at ScienceDirect

MethodsX

journal homepage: www.elsevier.com/locate/mex

Method Article

Controlled photogrammetry system for determination of volume and surface features in soils

Jared Suchan, Shahid Azam*

Environmental Systems Engineering, Faculty of Engineering and Applied Science, University of Regina, 3737 Wascana Parkway, Regina, SK S4S 0A2, Canada

A B S T R A C T

Quantitative and qualitative determination of total volume and surface features of a soil specimen is important in geotechnical engineering. Available methods suffer from a variety of shortcomings such as sample disturbance, equipment calibration, and lack of precision. The Controlled Photogrammetry System (CPS) is based on Structure-from-Motion (SfM) to capture a series of photographs and transform the images into a referenced three-dimensional model.

- This paper develops the Controlled Photogrammetry System.
- This paper describes the design and operation of the Controlled Photogrammetry System.
- This paper presents data processing and test results for a sand and clay.

A R T I C L E I N F O
Method name: Controlled Photogrammetry System
Keywords: Controlled photogrammetry system, Soil volume, Surface features, Structure from motion
Article history: Received 20 January 2021; Accepted 21 April 2021; Available online 28 April 2021

Specifications table

Subject Area:	Earth and Planetary Sciences
More specific subject area:	Land-Atmosphere Interactions
Method name:	Controlled Photogrammetry System
Name and reference of original method:	Structure-from-Motion [6]
Resource availability:	None

* Corresponding author.
E-mail address: shahid.azam@uregina.ca (S. Azam).

https://doi.org/10.1016/j.mex.2021.101368

Introduction

An accurate determination of surface features and total volume is critical in geotechnical engineering. Quantitative information is used in phase relationships whereas qualitative assessment are important to identify undulations and cracks in soils. Both of these data sets undergo changes because of variation in the amount of water in the soil. Several methods have been developed to determine surface features and total volume in soils. The mesh-and-probe method was developed by Khan and Azam [5] to manually capture three-dimensional (3D) variation in swelling of expansive clays using up to 800 measurements. The main shortcomings of this method are the large time requirement, potential sample disturbance, and lack of precision. Likewise, the camera-and-laser scanning methods have been developed by Auvray et al. [2] and Jain et al. [4] to automatically capture

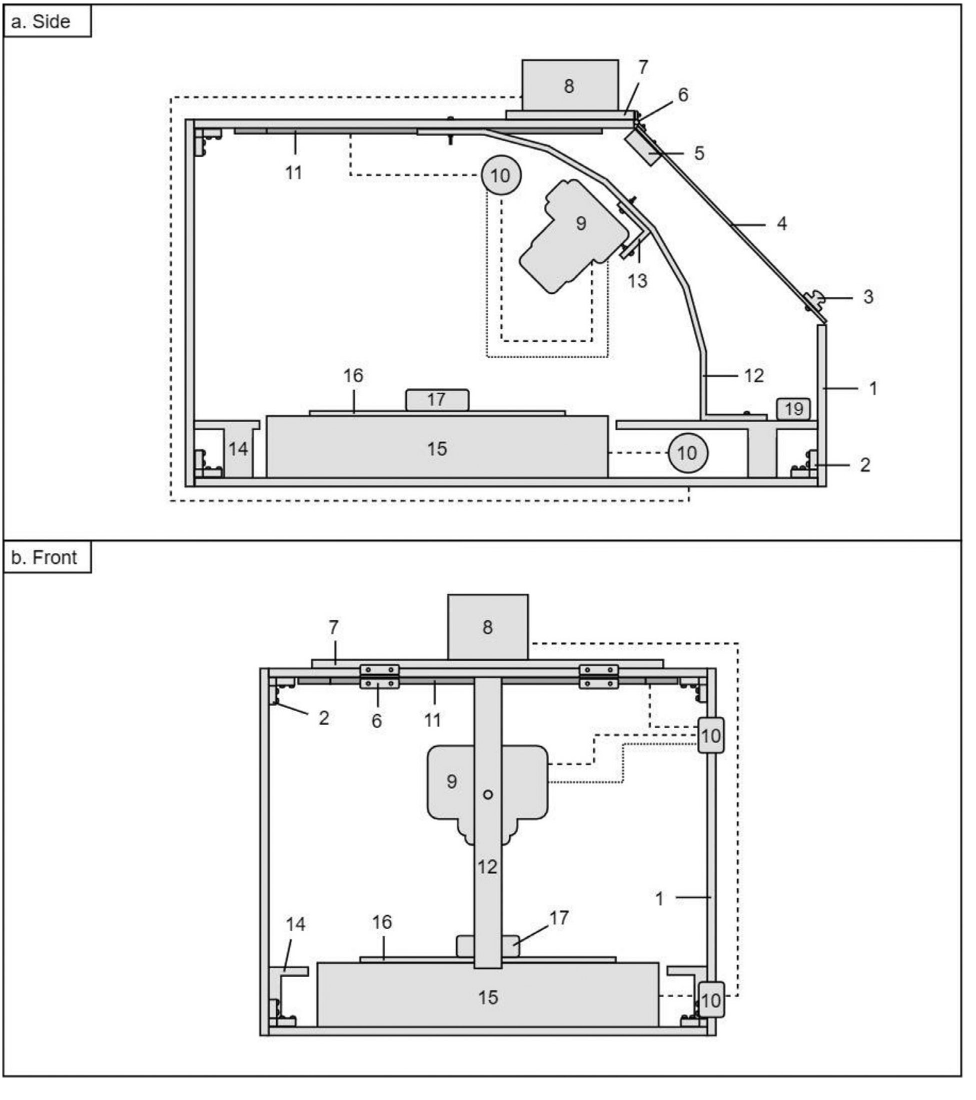

Fig. 1. Schematic of the CPS: (a) view from the left-side, and (b) view from the front.

shrinkage and crack formation in soils. This method is limited by a need for sophisticated calibration and expensive equipment. Li and Zhang [6] introduced a low-cost, non-contact method to measure the volume of unconstrained clay samples using a simple equipment. Based on Structure-from-Motion (SfM), this method creates accurate 3D models by photographing the sample from multiple viewpoints and angles.

This paper develops a Controlled Photogrammetry System (CPS) based on an improved version of the SfM method to capture quantitative and qualitative features of soil contained in a cup. The main aspects of CPS include the following: (i) low evaporative losses by using a sealed housing; (ii) improved photographic conditions by using fixed lighting; (iii) improved inter-modelling consistency by using fixed camera mount angles; and (iv) increased photo capture rate by using a modified rotating stand. After presenting the detailed design, the operational procedure is provided using a stepwise approach to collect imagery for modelling. Next, a guide for data processing and analysis is provided for various modes of volume changes in soil. Finally, quantitative and qualitative assessments of sand and clay in wet and dry states is provided to validate the accuracy and the precision of the method.

Detailed design

Fig. 1 presents a schematic of the CPS and Table 1 lists the relevant components. The sealed housing reduces evaporative losses by inhibiting air flow and allows visual observation of the photo capturing process through the acrylic window. Inside the housing is a digital single-lens reflex (DSLR) camera, a rotating stand for the sample as well as a thermometer and a hygrometer to monitor temperature and humidity, respectively. There are three LED light fixtures affixed to the ceiling to ensure consistent lighting while reducing shadows around the sample. The DSLR camera is fastened to a mount that connects to the camera bracket. This arrangement results in five different orientation angles with respect to horizontal (5°, 20°, 35°, 50°, and 65°) as well as facilitates rapid movement of the DSLR camera between the orientation angles.

The photo capture is improved with the development of a semi-autonomous workflow. The camera is connected to a laptop equipped with an open-source control software (*digiCamControl2*) capable of capturing an image every 4 s. The camera settings are adjusted for optimum image quality using aperture, ISO, and shutter-speed. The aperture is set to the lowest value (focal ratio/25) to capture a large depth of field, thereby ensuring a simultaneous focus on both the specimen and surround targets. The ISO is set to the base value of 100 to ensure minimal grain and noise artefacts in the photos. Finally, the shutter-speed is set to a slower value of 1/10 to accommodate the reduced brightness caused by the choice of ISO setting.

Fig. 2 presents the target plate that is designed to sit on top of the rotating stand and Table 2 presents the target plate coordinates. The target plate contains 20-coded targets with 25 mm grid spacing thereby allowing the software to automatically identify the target points, locate common points between photographs, and generate an arbitrary coordinate system. The rotating stand is connected to a step controller that synchronizes the movement of the target plate with the intermittent photo capture. This precludes the possibility of blurry images associated with continuous sample movement. A unidirectional electric motor was installed to preclude any accidental change in the rotating direction.

Equipment operation and data processing and analysis

Fig. 3 presents a stepwise guide to operate the CPS. The soil sample is placed in the sealed housing and carefully orientated on the target plate. The camera settings are verified and the camera is put in the first position. The sample alignment is verified and adjusted if required. The photo capture is commenced and the step controller is started. After completing a full rotation, the camera to the next angle and the process is repeated.

Fig. 4 presents a visual guide to process and analyze the CPS data. To convert the photographs into a 3D triangulated mesh model, the computer software (*Agisoft Metashape Professional* (AMP)) was used. Processing involves uploading the photographs into a new project file in the software that, in

Table 1
Details of the CPS components.

Component, Make and Model (when required)	Dimensions (mm), Specifications (variable unit), Materials (when required)	Purpose	Comments and Limitations
1. Housing	L: 610; W: 295; H: 410; T: 19; M: Medium-Density Fibreboard	The PCD casing, built to contain the test sample and data collection sensors.	Enclosing the sample reduces evaporative loses during photograph collection, and reduces shadows around the sample.
2. Corner Brace Everbilt *859–755*	L: 50.8; H: 50.8; M: Steel	Supports the housing walls.	Connects to the housing walls in the corners.
3. Lid Handle Everbilt *859–116*	L: 124	Allows the window to be opened.	
4. Window Optix *11G0670A*	L: 430; W: 295; T: 2; M: Acrylic	Allows the data collection process to be observed without opening the housing.	
5. Window Brace	L: 300; W: 25; H: 15; M: Spruce	Provides a mounting point for the hinge to connect to the window.	
6. Hinge Everbilt *859–432*	L: 38; M: Brass Plated Steel	Allows the window to be opened to access inside the housing.	Attaches to the window and roof braces.
7. Roof Brace	L: 400; W: 180; T: 19; M: Medium-Density Fibreboard	Provides a mounting point for the hinge to connect to the housing.	
8. Step Controller Inkbird *IDT-E2RH*	L: 75; W: 85: H: 35	Provides cyclical power to the rotating stand, keeping the sample still for each photographic interval.	Turn = 1 second; Pause = 6 s.
9. Camera Nikon *D3000*	L: 126; W: 97; H: 65; S: 10.2 MP	Captures high-resolution images required for SfM processing.	F-number = 22; Shutter speed = 1/10. Sample cannot be moving during photo capture, else blurring occurs.
10. Cable Port	D: 50	Allows cables to pass through the housing.	
11. Lights Lampaous *B07KYKDV7S*	L: 300; W: 30; T: 6; C: 6000 K	Provides consistent lighting around the sample, limiting the occurrence of shadows.	
12. Camera Bracket	L: 275; W: 25; H: 250; T: 5; M: Steel	Consistently positions the camera in different orientation angles above the sample.	Fabricated by cutting a flat of steel into segments and welding together at 15° angles. Mounting holes drilled afterwards.
13. Camera Mount Everbilt *859–704*	L: 38; W: 38; H: 13; T: 3; M: Steel	Positions the camera on the bracket.	Connected using screws and nuts.
14. Floating Base	L: 290; W: 275; T: 19; M: Medium-Density Fibreboard	Sits nearly flush with the surface of the rotating stand and provides a mounting point for the camera bracket.	
15. Rotating Stand Fotonic *B01M5HN2AU*	D: 250; T: 38; R: 1.6 RPM	Rotates the sample to into a new position at each photographic interval.	Requires electric motor to be replaced with a unidirectional model.
16. Target Plate	D: 20; T: 3	Coded targets provide a means to generate an arbitrary coordinate system around the sample.	

(*continued on next page*)

Table 1 (*continued*)

Component, Make and Model (when required)	Dimensions (mm), Specifications (variable unit), Materials (when required)	Purpose	Comments and Limitations
17. Sample Container Humboldt *H-4256*	Top ID: 45.0; Bottom ID: 40.0; H: 13.5; T: 1.0; V: 19,217 mm^3; C: 14.3 $W{\cdot}m^{-1}{\cdot}{}^{\circ}K^{-1}$; M: Monel Nickel-Copper Alloy 400 Steel	Hosts sample material.	
18. Laptop ASUS *E406M*	L: 447; W: 326, H: 226; IV: 110 V	Connects to camera and controls shutter operation using DigiCam2 software.	
19. Environment Sensor Inkbird *IBS-TH1*	D: 104; H: 28	Logs temperature and humidity data.	Data logs extracted using cellphone Bluetooth.

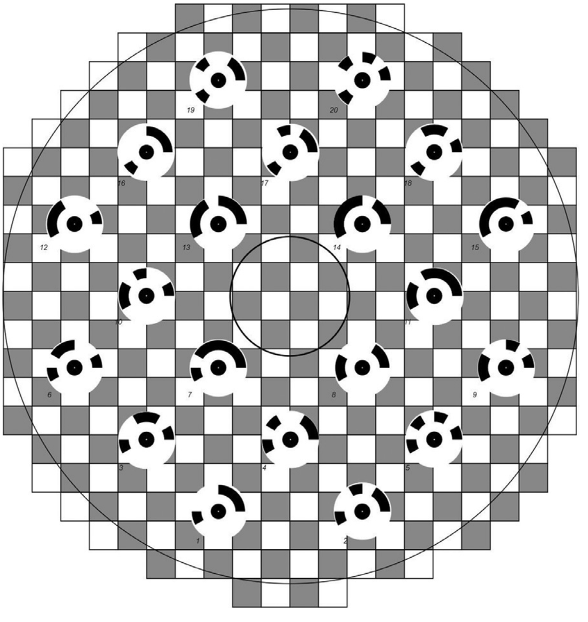

Fig. 2. Target plate template, placed on rotating stand beneath the sample container.

turn, aligning the photos, calculates depth maps, detect coded targets, and assembles a mesh model. A model of the sample cup is created in *Google SketchUp* (GSU) to establish the internal dimensions.

The mesh model is refined depending on contact with the sample cup. For the wall contact case, the triangulated mesh is cropped in *CloudCompare V.2* (CC2) along the rim of the sample cup. This mesh along with the sample cup model is imported into *Autodesk Civil 3D* (AC3) to determine the intersection line between the two models. This line is used in *CloudCompare V.2* (CC2) to obtain the soil model. For the no wall contact case, the perimeter line of the soil is drawn on the triangulated mesh in *Agisoft Metashape Professional* (AMP). This line is brought into *Google SketchUp* (GSU) along with the sample cup interior model. To capture the sample sides, the perimeter line is extended downwards to create a vertical surface that completely joins the cup. Finally, the model is brought into *CloudCompare V.2* (CC2) and cropped using the perimeter line.

Table 2
Coordinates for the coded target plate.

Target Number	X (mm)	Y (mm)
1	75	25
2	125	25
3	50	50
4	100	50
5	150	50
6	25	75
7	75	75
8	125	75
9	175	75
10	50	100
11	150	100
12	25	125
13	75	125
14	125	125
15	175	125
16	50	150
17	100	150
18	150	150
19	75	175
20	125	175

Table 3
Quantitative assessment of sand and clay samples in wet and dry states.

Property	Sand		Clay	
	Wet	Dry	Wet	Dry
Number of Photographs	310	381	369	377
Time (min)	28	34	32	35
Capture Rate (photos/min)	11.0	11.2	11.5	10.8
Control Points RMSE (mm)	0.38	0.44	0.32	0.58
Reprojection Error (pix)	0.629	0.494	0.626	0.290
Temperature (°C)	21.2	20.8	20.9	22.4
Humidity (%)	32.5	31.7	33.8	24.1
Volume (mm^3)	15,663	15,848	16,482	15,319
Surface Area (mm^2)	1754	1731	1622	2233

The data is analyzed using *CloudCompare V.2* (CC2). The sample model and the cup model are converted to point clouds (1×10^6 points) and loaded into the 2.5D Volume tool. The sample point cloud is designated the 'surface', while the cup point cloud is designated the 'ground'. The volume tool utilizes a rasterization process to create cells that connects both point clouds, and then measures the height difference of each cell. The reported volume is equal to the summed contribution of all the cells. Volume is computed from the difference between the two clouds. For the wall contact case, the exposed surface area is determined by applying the Mesh Surface Area tool only to the cropped surface area model whereas this tool is also applied to the vertical surface model for the no wall contact case.

Sample preparation and test results

Two soils were selected to determine volume and surface features: a fine sand that remains unchanged with varying water content and a highly plastic clay that shrinks and swells with varying water content. The soil samples were prepared by adding water and allowing the mix to saturate in a jar for 24 h and transferred to the sample cup for photo capture in CPS. Thereafter, the samples were oven dried at 110 °C for24 h and the process was repeated.

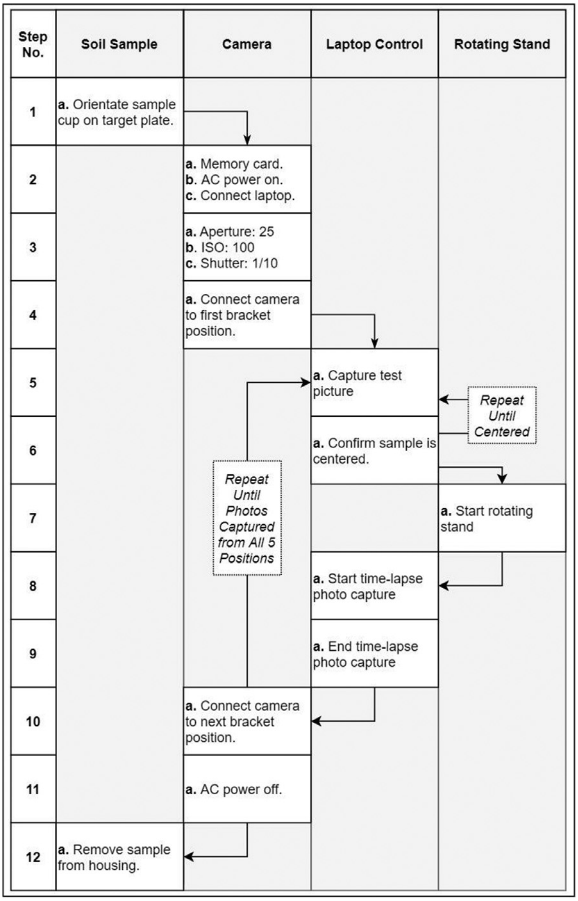

Fig. 3. Stepwise guide to operating the CPS.

Fig. 5 shows photographs of the sand and clay samples in wet and dry states and Table 3 presents a quantitative assessment of the CPS measurements. Each test required approximately 30 min to capture about 350 images. The root mean square error (RMSE) of the target points is a quantitative measure of accuracy that evaluates retransformation of the model coordinate system in the X, Y, and Z directions [1]. The RMSE was found to range from 0.32 mm to 0.58 mm indicating a close match between target points and the retransformed model. The reprojection error evaluates the calibration process and reflects the quality of images and the number of well-placed control targets [7]. The reprojection error (threshold of 1 pix) ranged from 0.290 to 0.629 pix indicating that the 3D points in the models closely recreate the true projection [3]. The difference in both volume and area between the wet and the dry states for sand samples was found to be 1%. This means that the method can precisely conduct quantitative evaluations. In contrast, the clay volume decreased by 1164 mm^3 (−7%) when the wet state is compared with the dry state. The exposed surface area increased by 611 mm^2 (27%) as the sides detached from the cup walls due to lateral and vertical shrinkage.

Fig. 6 presents a qualitative assessment of the surface features. The wet sand had a stippled appearance whereas the wet clay had a smooth appearance such that both samples touched the walls of the cup. When dried, the sand appeared to have negligible change whereas the clay shrunk both vertically and laterally and was pulled away from the cup walls. While no desiccation cracks

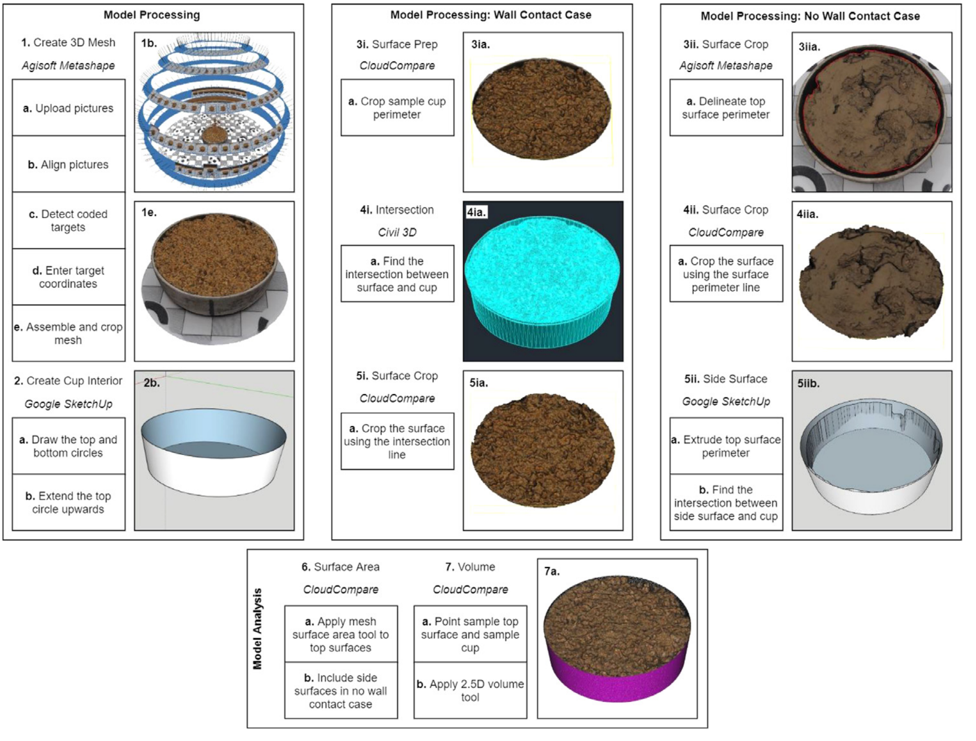

Fig. 4. Visual guide to processing and analyzing data.

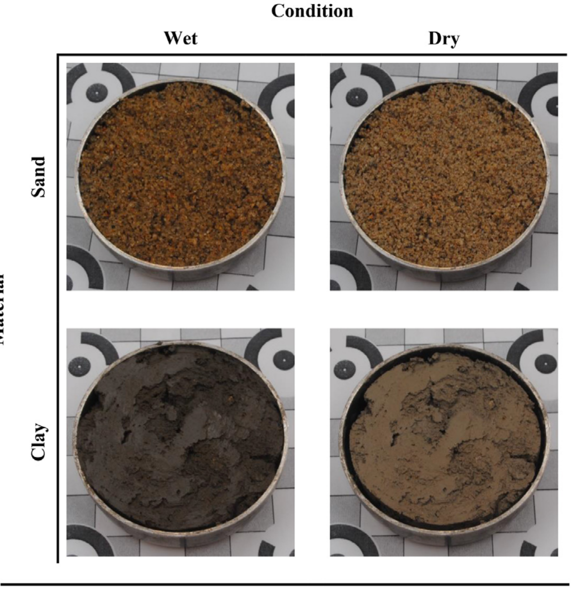

Fig. 5. Photographs of sand and clay samples in wet and dry states.

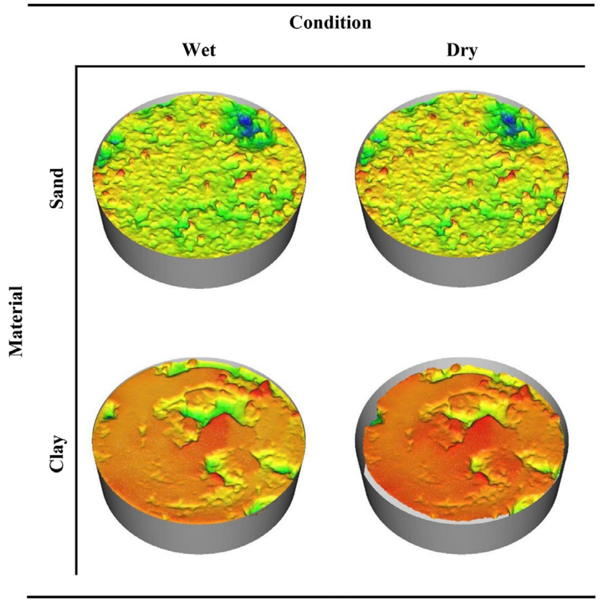

Fig. 6. Qualitative assessment of sand and clay samples in wet and dry states.

were observed on the dried clay sample, Li and Zhang [6] demonstrated that the SfM is capable of characterizing such features.

Acknowledgment

Natural Sciences and Engineering Research Council of Canada for providing financial support.

Declaration of Competing Interest

The authors declare that they have no known competing financial interests or personal relationships that could have appeared to influence the work reported in this paper.

References

[1] F. Agüera-Vega, F. Carvajal-Ramírez, P. Martínez-Carricondo, Accuracy of digital surface models and orthophotos derived from unmanned aerial vehicle photogrammetry, J. Surv. Eng. 143 (2) (2017) 04016025.
[2] R. Auvray, S. Rosin-Paumier, A. Abdallah, F. Masrouri, Quantification of soft soil cracking during suction cycles by image processing, Eur. J. Environ. Civ. Eng. 18 (1) (2014) 11–32.
[3] S. Barba, M. Barbarella, A. Di Benedetto, M. Fiani, L. Gujski, M. Limongiello, Accuracy assessment of 3D photogrammetric models from an unmanned aerial vehicle, Drones 3 (4) (2019) 79.
[4] S. Jain, Y.H. Wang, D.G. Fredlund, Non-contact sensing system to measure specimen volume during shrinkage test, Geotech. Test. J. 38 (6) (2015) 936–949.
[5] F. Khan, S. Azam, Spatial variability in swelling of aggregated expansive clays, Innov. Infrastruct. Solut. 1 (1) (2016) 1–6.
[6] L. Li, X. Zhang, A new approach to measure soil shrinkage curve, Geotech. Test. J. 42 (1) (2019) 1–18.
[7] G. Percoco, F. Lavecchia, A.J.S Salmerón, Preliminary study on the 3D digitization of millimeter scale products by means of photogrammetry, Proc. CIRP 33 (2015) 257–262.